Microelectronic Engineering 86 (2009) 1190–1193

Contents lists available at ScienceDirect

Microelectronic Engineering

journal homepage: www.elsevier.com/locate/mee

Analysis of MEMS mechanical spring for coupling multimodal micro resonators sensor

Nor Hayati Saad *, Raya K. Al-Dadah, Carl J. Anthony, Michael C.L. Ward

University of Birmingham, School of Mechanical Engineering, Edgbaston, B15 2TT Birmingham, UK

ARTICLE INFO

Article history:
Received 29 September 2008
Received in revised form 26 November 2008
Accepted 27 November 2008
Available online 10 December 2008

Keywords:
Butterfly shaped MEMS spring
Coupled micro resonator array sensor
Finite element analysis

ABSTRACT

This paper introduces a new butterfly shaped mechanical spring used to couple an array of five micromechanical resonating mass balance sensors, which are been developed for advanced applications in detecting chemical and biological species. The sensors were fabricated using a 5 μm SOI (silicon on insulator) wafer. The performance of the spring is analysed using finite element analysis (FEA) and compared with other potential designs. From the analysis the butterfly spring provides enhanced response amplitude along the excitation axis and a balanced displacement for sensitivity of mass detection. Additionally, the overall frequency bandwidth is easily controlled to suit the application.

1. Introduction

Mechanical springs are often employed in MEMS applications to couple devices together for various applications. Mechanical springs were used to couple two resonators [1,2] and also in 2D resonator arrays for MEMS filters [3]. Springs have also been used for high performance probing [4], MEMS transducers [5] and supporting oscillating masses in micro vibratory rate gyroscope [6]. This paper introduces a closed loop butterfly shape spring which is used to couple five resonant micromechanical mass balance sensors together. The Coupled Micro Resonator Array (CMRA) sensor has been developed for advanced application in detecting different chemical and biological species presence in gaseous or liquid environments [7]. To simplify the complexity of sensor structure and the associated signal processing system the CMRA was designed with just two connections; an input and an output port. The state of each of the sensors can then be monitored by measuring the modal resonant frequencies of the coupled system at the output end of the coupled array. Fig. 1a shows a schematic of the CMRA sensor structure. The structure consists of five fixed–fixed beam resonators (sensor element), comb drive actuator, and mechanical spring to couple the resonators.

The operation of the CMRA depends on the response pattern of the five modal frequencies of the coupled resonators. This pattern can then be used as a signature to determine the amount and type of mass adsorbed on to each of the individual resonators [7,8]. Each of the modal frequencies signifies an eigenmode of oscillation of the coupled resonator in the lateral direction along the excitation axis (*Y*-axis). To ensure the sensor system works effectively, the mechanical springs must be designed so as not to introduce any unwanted eigenmodes within the main modal frequencies of the coupled structure. The performance of the sensors mainly depends on the displacement of the sensor element in *Y*-axis. Therefore, the spring must be more flexible along the excitation axis (*Y*-axis) and rigid in *X*-axis. Overall frequency bandwidth of the response depends on the mechanical coupling [9] between each resonator. The spring should be designed, so that the stiffness can be controlled easily by configuring the design parameters of the spring. To date most of the existing micro springs reported in the literature [1–6], [10] do not meet these requirements. For example with simple zigzag shape spring (Fig. 1b), the spring may introduce spurious responses due to torsion and elongation of the spring element in *X*-axis during the operation. As a consequence the response amplitude (*Y*-axis) of the sensors may be reduced.

2. Design concept

In order to study the performance of the spring in coupling the resonant sensors, each of the resonators was designed with a constant mass, total length (L) of 700 μm and 3 μm width (b) as shown in Fig. 2a. The shuttle length (L_s) and width (b_s) is 200 and 10 μm, respectively. The stiffness of the resonator (k_b) is 2.9 N/m and its natural frequency (f_R) is 48.760 kHz. To be compatible with standard measurement facilities, the modal frequency of the coupled structure was set around 50 kHz. Fig. 2a is a schematic diagram of the butterfly spring design. The spring was designed with joined-tilted beams in order to increase the displacement of the

* Corresponding author. Tel.: +44 (0) 121 414 4226; fax: +44 (0) 121 414 3958.
E-mail address: nhs621@bham.ac.uk (N.H. Saad).

0167-9317/$ - see front matter © 2008 Elsevier B.V. All rights reserved.
doi:10.1016/j.mee.2008.11.092

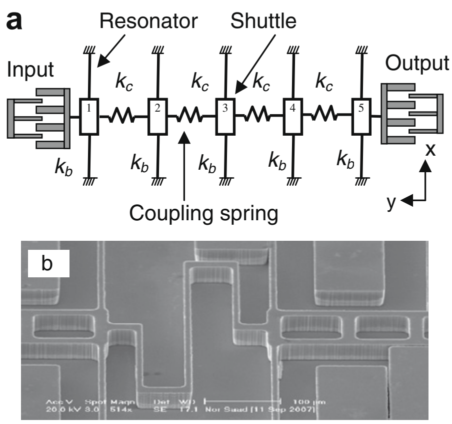

Fig. 1. (a) Schematic of Coupled Micro Resonator Array (CMRA) Sensor; (b) zigzag spring.

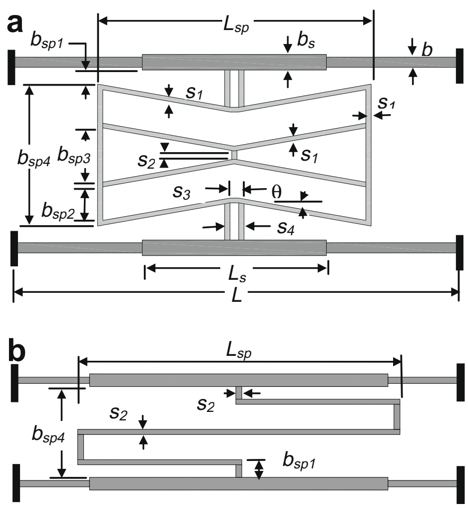

Fig. 2. (a) Schematic of the Butterfly Spring; (b) zigzag shape spring.

springs along the excitation axis. Any possibilities of the torsion and elongation of the spring elements in *X*-axis are reduced by fixing the middle of the spring structure. In analysing the eigenfrequencies, eigenmodes and the effect of coupling stiffness on the frequency bandwidth of the response of the coupled system, three designs of the butterfly spring with varied coupling stiffness were considered; sp1(k_c = 0.1149 N/m), sp2(k_c = 0.2228), and sp3(k_c = 0.6746). The stiffness of the spring was adjusted by varying the length (L_{sp}) and the width of the spring (b_{sp}).The other parameters were fixed: S_1 = 1 μm; S_3 = 10 μm; S_4 = 12 μm; θ = 11°; and b_{sp2} = 53 μm. The effect of coupling the resonators with three zigzag springs sp4, sp5, and sp6 (Fig. 2b) was also investigated for comparison. The spring sp4, sp5, and sp6 were designed

Table 1
Design parameters of the coupling spring (sp) (all dimensions in μm unit).

sp	S_2	L_{sp}	b_{sp1}	b_{sp4}	Mass (ng)	k_b:k_c
sp1	10.7	312.0	23.0	182	21.3	25.6:1
sp2	10.9	250.0	29.0	170	18.1	13.2:1
sp3	10.5	175.0	36.5	155	14.2	4.4:1
sp4	2.5	358.0	25.5	121	24.2	25.6:1
sp5	2.5	282.5	25.5	121	19.8	13.3:1
sp6	2.5	187.0	25.5	121	14.3	4.3:1

Table 2
Eigenfrequency analysis result [kHz].

sp	Modal frequency of single spring (f_{sp}) and coupled resonators (f_M)					
	f_{sp}	f_{M1}	f_{M2}	f_{M3}	f_{M4}	f_{M5}
sp1	29.9	48.2	48.6	49.4	50.2	50.8
sp2	44.5	51.2	52.7	55.8	58.3	59.9
sp3	84.5	39.9	43.6	49.8	56.4	62.2
sp4	54.1	33.5	35.2	38.1	42.1	44.9
sp5	80.6	37.1	39.5	43.3	47.3	49.7
sp6	154.5	40.8	44.8	51.5	58.9	64.5

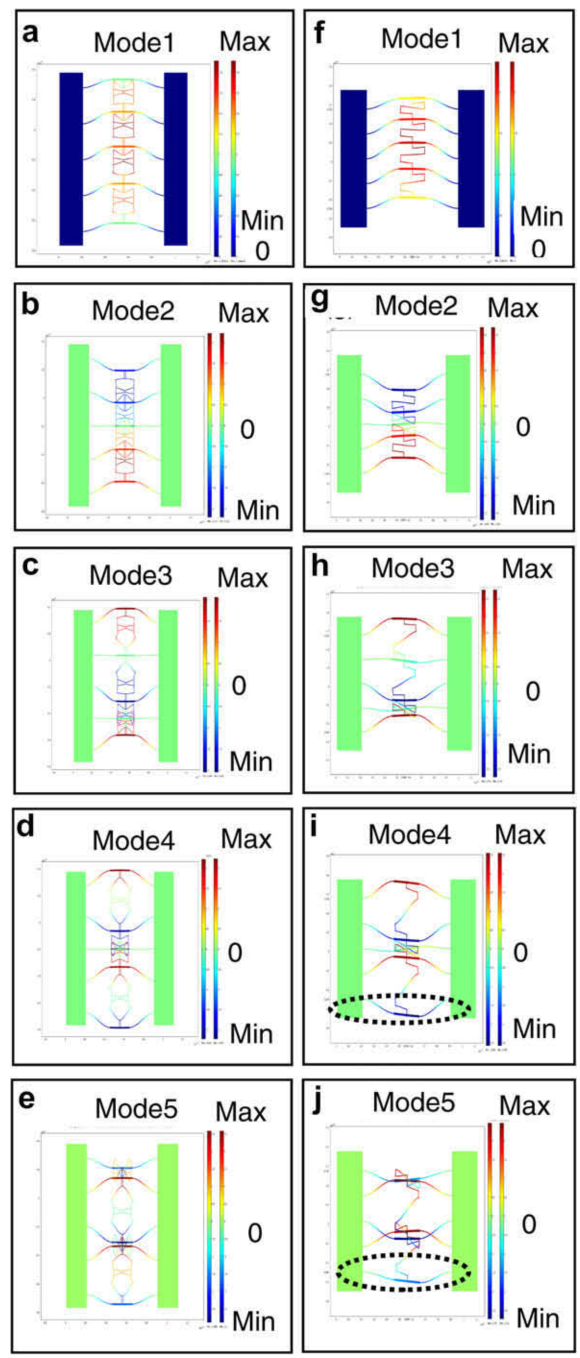

Fig. 3. Eigenmodes (at k_b:k_c = 4:1); (a)–(e) structure coupled with closed butterfly spring (sp3); (f)–(j) structure coupled with zigzag spring (sp6), (Note: elements which highlighted with dotted line are example of unbalanced displacement due to torsion and elongation of zigzag spring element).

to have a comparable coupling stiffness with the first three butterfly spring, respectively ($k_{c(sp4)} = 0.1148$ N/m, $k_{c(sp5)} = 0.2216$, and $k_{c(sp6)} = 0.6801$). Refer to Table 1 for details of the design parameter.

3. Finite element analysis

All analyses (eigenfrequency, static and parametric; and frequency response analysis) were performed using COMSOL Multiphysics, finite element analysis (FEA) software [11]. Eigenfrequency analysis was performed to determine the natural frequency (f_{sp}) of the spring, modal frequencies of the coupled resonators (f_M) and the eigenmodes of the structure [7,11]. The stiffness of the coupling springs was analysed using static and parametric analysis. The static deflection in *Y*-axis of the six springs was compared when up to 10 μN force was applied on the spring along the *Y*-axis. The static deflection in *X*-axis also was compared in observing the rigidity of the spring along the axis. Finally, frequency response analyses were conducted on the butterfly spring to examine the overall pattern of the frequency bandwidth, separation of the modal frequencies and the response amplitude of the coupled resonators. The software solves the frequency response, for steady state harmonic excitation with an excitation frequency, f within the range between the first and fifth modes of the natural frequency of the system as determined by the eigenfrequency analysis.

4. Result and discussion

4.1. Eigenfrequency and eigenmodes

Table 2 shows the natural frequency of the coupling springs, f_{sp} and the five modal frequencies of the coupled resonators, f_M. The five modal frequencies of the coupled resonators rely on the mass and the stiffness of the coupling spring. For example when the resonators ($f_R = 48.760$ kHz) were coupled with sp2 with 44.5 kHz natural frequency the modal frequencies of the structure increased to 51.2 for mode 1 (f_{M1}), 52.7 (f_{M2}), 55.8 (f_{M3}), 58.3 (f_{M4}), and 59.9 (f_{M5}). From the eigenmode analysis of the coupled structure (Fig. 3a–j), both springs portray similar response pattern for each of the modes. The resonators were effectively coupled by both types of springs. However, it can be depicted that the displacement of the resonators which were coupled with zigzag spring (Fig. 3g–j) is unbalanced due to torsion and elongation of the unbalanced spring element. This unbalanced displacement may reduce the sensor performance and sensitivity of mass detection.

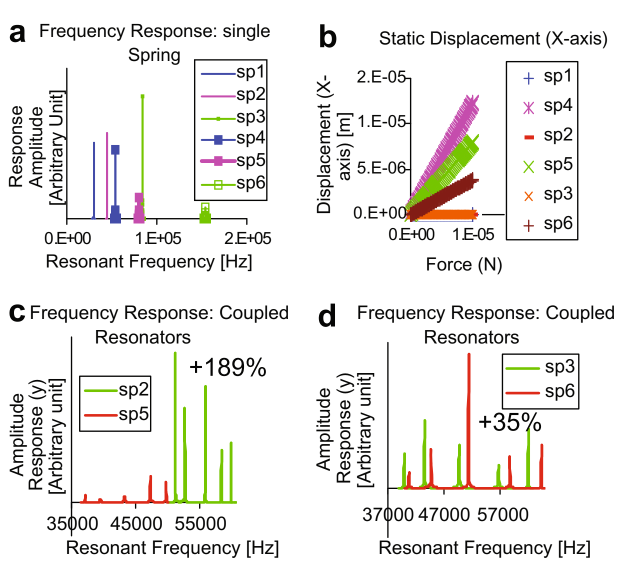

Fig. 4. (a) Frequency response of single spring; (b) static displacement of the spring (*X*-axis); (c) and (d) frequency response of the five coupled resonators.

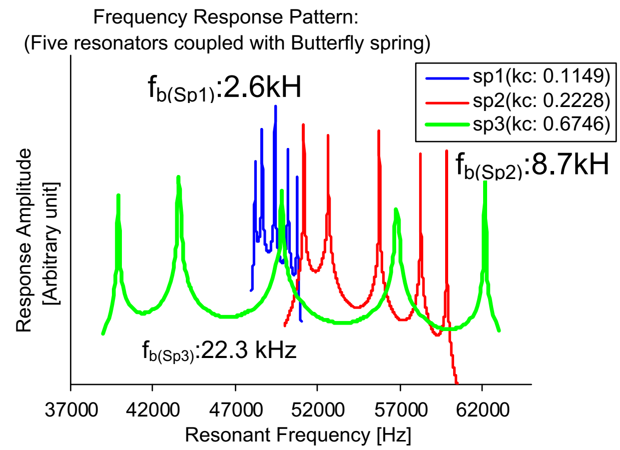

Fig. 5. Frequency response pattern of the resonant sensors coupled with butterfly spring.

4.2. Static and frequency response analysis

At a comparable coupling stiffness for both springs (sp1//sp4, sp2//sp5, and sp3//sp6) the butterfly spring provides higher response amplitude compared to zigzag spring as portrayed in Fig. 4a. With closed loop butterfly shape design, the spring is more rigid in *X*-axis (Fig. 4b). Therefore, it offers more balanced oscillation to enhance the displacement in *Y*-axis.

Fig. 4c and d illustrate example of overall frequency response pattern of the five coupled resonators. If we compared the response amplitude of the two types of springs at the fifth mode, the response amplitude of the sp2 and sp3 are higher compared to sp5 and sp6 with more than 189% and 35%, respectively. The less response amplitude of the structure coupled with zigzag spring is expected due to twisted resonators cause by the unbalanced torsion and elongation of the spring element as discussed in eigenmodes analysis. Fig. 5 shows the response pattern of the resonators coupled with butterfly spring. By controlling the stiffness of the coupling spring the overall frequency bandwidth and separation of modal frequency can be easily adjusted to suit with the application. For example by reducing the coupling stiffness from 0.6746 to 0.1149 N/m the overall frequency bandwidth decreased from 22.3 (sp3) to 2.6 kHz (sp1).

5. Conclusion

From analysis it is found that the new butterfly shaped spring provides better performance in coupling the resonant sensors. The butterfly spring obtained higher response amplitude with balanced displacement along the excitation axis (*Y*-axis) and reduced unwanted response within the five modal frequencies which enhanced readability of the output signal. The butterfly spring is more flexible in *Y*-axis and rigid in *X*-axis due the spring design itself where the joined-tilted beams were fixed at the middle. With more balanced displacement of the spring in *Y*-axis and without twisting any resonators element, it will provide better sensitivity for mass detection. By properly configuring the design parameters of the butterfly spring, the coupling stiffness can be more easily controlled in order to adjust the separation of the modal frequencies and overall frequency bandwidth to suit with the application.

References

[1] Y. Gurbuz, M. Parlak, T.F. Bechteler, A. Bozkurt, Sensors and Actuators (2005) 38–47.
[2] M. Naseer, M. Parlak, T. Bechteler, Y. Gurbuz, Nanotechnology (2003) 388–391.
[3] D. Weinstein, S.A. Bhave, M. Tada, S. Mitarai, K. Ikeda, IEEE (2007) 1362–1365.
[4] J.M. Haemer, S.K. Sitaraman, D.K. Fork, F.C. Chong, S. Mok, D.L. Smith, F. Swiatowiec, 50th Electronic Components and Technology Conference (2000) 1157–1163.
[5] D. Ozevin, S. Pessiki, A. Jain, D.W.Greve, A.J. Oppenheim, http://www.ece.cmu.edu/~dwg/research/spieaefinal.pdf.
[6] Kyu-Yeon Park, Chong-Won Lee, Yong-Su Oh, Young-Ho Cho, Sensors and Actuators A (Physical) A64 (1) (1998) 69–76.
[7] Nor Hayati Saad, Michael C L Ward, Raya Al-Dadah, Carl Anthony, Baskar Choubey, Steve Collins, Eurosensors (2008) 60–63.
[8] Bhaskar Choubey, Steve Collins, Nor Hayati Saad, Michael C L Ward, Eurosensors (2008) 52–55.
[9] P.J. Stephanou, G. Piazza, C.D. White, M.B.J. Wijesundara, A.P. Pisano, Journal of Physics: Conference Series 34 (2006) 342–349.
[10] K. Miyamoto, T. Jamori, K. Sugano, O. Tabata, T. suchiya, Sensors and Actuators (2008) 136–142.
[11] COMSOL Multiphysics, Structural Mechanics Module, User's Guide, Version 3.